Earth and Planetary Science Letters 600 (2022) 117875

Contents lists available at ScienceDirect

Earth and Planetary Science Letters

journal homepage: www.elsevier.com/locate/epsl

Spatiotemporal variation of Li isotopes in the Yarlung Tsangpo River basin (upper reaches of the Brahmaputra River): Source and process

Jun-Wen Zhang [a,b], Ya-Ni Yan [a], Zhi-Qi Zhao [a,*], Xiao-Ming Liu [c], Xiao-Dong Li [b], Dong Zhang [d], Hu Ding [b], Jun-Lun Meng [e], Cong-Qiang Liu [b,*]

[a] School of Earth Science and Resources, Chang'an University, Xi'an 710054, China
[b] Institute of Surface-Earth System Science, Tianjin University, Tianjin 300072, China
[c] Department of Earth, Marine and Environmental Sciences, University of North Carolina, Chapel Hill, NC 27599-3315, USA
[d] School of Resource and Environment, Henan Polytechnic University, Jiaozuo, China
[e] State Key Laboratory of Environmental Geochemistry, Institute of Geochemistry, Chinese Academy of Sciences, Guiyang 550081, China

ARTICLE INFO

Article history:
Received 28 June 2022
Received in revised form 10 October 2022
Accepted 17 October 2022
Available online 27 October 2022
Editor: A. Jacobson

Keywords:
lithium isotopes
chemical weathering
geothermal water
isotopic fractionation
Tibetan Plateau

ABSTRACT

The increase in marine Li isotope composition (δ^7Li, ~9‰) since the Cenozoic is possibly related to continental chemical weathering associated with tectonic uplift (e.g., the Tibetan Plateau [TP]). However, the reasons for the spatiotemporal variations of δ^7Li in the rivers flowing through the TP are still under debate, hindering the understanding of the changes in seawater δ^7Li. Herein, various geological samples, i.e. river waters, river suspended particulate materials, river sediments, hot springs and silicate rocks, from the Yarlung Tsangpo River basin, the largest river system in the TP, have been analyzed to understand the source and isotopic fractionation of dissolved Li in rivers flowing through high-altitude and tectonic regions. The Yarlung Tsangpo River has an unusually high dissolved Li concentration ($[Li]_{dis}$) (0.5–313 μg/L, mean 58.4 μg/L, $n = 93$) and low δ^7Li_{dis} values (+1.0‰–+14.7‰, mean +6.4‰, $n = 92$) compared with most river waters. These results can be explained by the input of geothermal water with extremely high $[Li]_{dis}$ (5.5–34.4 mg/L, mean 15.7 mg/L, $n = 9$) and low δ^7Li_{dis} (−1.7‰–+3.1‰, mean +1.0‰). Silicate weathering is probably responsible for elevated δ^7Li_{dis} in river water compared to geothermal water, but the binary mixture model results of silicate weathering and geothermal water do not support this speculation. Ongoing Li isotope fractionation between dissolved loads and secondary minerals has been suggested to be the main reason for the increased δ^7Li_{dis} in river water. Field study and adsorption experiment results support the view of continuous Li isotope fractionation in rivers. Physical erosion and chemical weathering processes that provide fresh secondary minerals to rivers as well as dissolved Li from geothermal water transported in rivers over long residence times promote Li isotope fractionation. Hence, with the emergence of a continental geothermal system, the tectonic activity may directly or indirectly induce the simultaneous increase in dissolved Li flux and δ^7Li_{dis} in rivers that eventually flow into the ocean. This can partially explain the increase in seawater δ^7Li in the Late Cenozoic.

1. Introduction

The uplift of the Himalayas has been affecting the regulation of the Earth's climate since the Cenozoic. This accelerates the chemical weathering of silicates and sequesters atmospheric CO_2 through the deposition of carbonates in the ocean (Raymo and Ruddiman, 1992). Early studies have suggested that the variation in the isotopic compositions of Sr ($^{87}Sr/^{86}Sr$) and Os ($^{187}Os/^{186}Os$) in seawater provides important clues to silicate weathering during this period, but this has been challenged by alternative interpretations such as meta-carbonate and black shale weathering (e.g., Galy et al., 1999). Lithium (Li) and its isotopes are potentially excellent tracers of silicate weathering processes because of following reasons. Li is almost exclusively hosted in silicate minerals with low abundance in carbonates. In addition, Li has remarkable isotopic fractionation during low-temperature water-rock reactions and its geochemical behavior and isotopic composition are not directly affected by redox reactions or biological processes (Penniston-Dorland et al., 2017 and references therein). Lastly, the increase in seawater Li isotope ratios (δ^7Li, approximately 9‰) since the

* Corresponding authors.
E-mail addresses: zhaozhiqi@chd.edu.cn (Z.-Q. Zhao), liucongqiang@tju.edu.cn (C.-Q. Liu).

https://doi.org/10.1016/j.epsl.2022.117875
0012-821X/

Cenozoic may be linked to the changes in continental chemical weathering intensity and secondary mineral formation associated with the tectonic uplift of the Himalayas (Misra and Froelich, 2012; Li and West, 2014; Wanner et al., 2014; Pogge von Strandmann and Henderson, 2015; Caves Rugenstein et al., 2019).

Riverine dissolved Li flux and its isotopic composition (δ^7Li_{dis}) regulate the variation in Li isotope composition in seawater (Misra and Froelich, 2012; Li and West, 2014; Vigier and Goddéris, 2015). Study results from modern rivers may provide some insights into the evolution of δ^7Li_{dis} in seawater and its relationship with chemical weathering (e.g., Pogge von Strandmann and Henderson, 2015; Dellinger et al., 2015). Thus, numerous studies have focused on the mechanisms or factors influencing Li isotope fractionation during chemical weathering in the catchment (e.g., Huh et al., 1998; Kısakürek et al., 2005; Dellinger et al., 2015; Liu et al., 2015; Wang et al., 2015; Pogge von Strandmann et al., 2017; Murphy et al., 2019; Weynell et al., 2021). The consensus is that dissolved Li in rivers is predominantly derived from silicate weathering, and chemical weathering is the main influence on riverine δ^7Li_{dis}. Nonetheless, δ^7Li_{dis} values in modern rivers globally show significant variation (from +1.2‰ to +43.7‰) (Penniston-Dorland et al., 2017) but the factors affecting this variation remain complex and debatable (e.g., Winnick et al., 2022). It has been proposed that these factors may be divided into process and source controls (e.g., Gou et al., 2019; Weynell et al., 2021). Process control emphasizes that lighter ^6Li tends to be incorporated into and/or adsorbed onto secondary minerals during weathering (e.g., Vigier et al., 2008), principally influenced by the ratio of primary rock dissolution to secondary mineral formation, water residence time, river suspended particulate material (SPM) concentration, as well as ambient pH and temperature (Wanner et al., 2014; Liu et al., 2015; Pogge von Strandmann et al., 2017; Gou et al., 2019). Source control mainly refers to some other Li-rich end members (e.g. evaporites or geothermal water) having a significant influence on the dissolved Li concentration ($[Li]_{dis}$) and isotopic composition of river water (Henchiri et al., 2014; Gou et al., 2019; Ma et al., 2020). Anthropogenic emissions may also influence the $[Li]_{dis}$ and δ^7Li_{dis} values in modern rivers (Choi et al., 2019), but have no effect on ancient rivers or seawater millions of years ago. Recently significant temporal δ^7Li_{dis} variations in water have been observed from the same river sample sites, mainly caused by both changes in sources and processes associated with seasonality (e.g., Hindshaw et al., 2019a; Gou et al., 2019; Zhang et al., 2022).

As the so-called 'water tower of Asia', the Tibetan Plateau (TP) is the source of many large rivers in Asia, namely the Yarlung Tsangpo River (YTR, the upper reaches of the Brahmaputra River), and the Ganges, Indus, Yellow, Yangtze, Salween, and Mekong Rivers, transporting large amounts of dissolved and suspended materials into the ocean. Previous studies have shown that these rivers have high $[Li]_{dis}$ compare to other large rivers worldwide with a mean value of 1.49 μg/L (Weynell et al., 2021). The abnormally high $[Li]_{dis}$ in the headwaters of the Yangtze River (eastern TP) is possibly mainly sourced from the dissolution of evaporites (Wang et al., 2015; Ma et al., 2020). However, Weynell et al. (2017) suggested that the high $[Li]_{dis}$ in the headwaters of rivers from the western TP, such as the YTR and Indus River, was not attributable to the dissolution of evaporites but to silicate weathering. Some studies have showed that some rivers with high $[Li]_{dis}$ in the TP regions were fed by Li-rich geothermal water (Kısakürek et al., 2005; Bohlin and Bickle, 2019). This is consistent with the recent finding that high levels of trace elements, including As, B, Cs, and Li in YTR river waters, are predominantly sourced from geothermal waters in the catchment, and that these element concentrations have significant seasonal variations (Zhang et al., 2021a). Thus, we suspect that the δ^7Li_{dis} value in some TP rivers may be considerably affected by the source rather than being exclusively controlled by silicate weathering processes. Currently, the influence of the source and process on spatial and seasonal variations in the Li isotope composition of river water in the TP is unclear (Weynell et al., 2017, 2021; Ma et al., 2020), which prevents the understanding of the relationship between chemical weathering in tectonic regions and their Li isotope compositions.

Geological samples have been collected from river waters in the YTR basin – the largest river system in the TP. The objective of this study is to understand the geochemical behavior of Li and its isotopes during riverine transportation, and determine the factors affecting the spatiotemporal variations of δ^7Li_{dis} in the YTR. These results help understand the potential causes of variation in δ^7Li_{dis} in these rivers and understand the relationship between tectonic uplift and the evolution of Li isotope composition in seawater over the Cenozoic.

2. Study area

As mentioned above, the YTR is the largest river system in the TP that flows through high-altitude mountains at an average elevation of about 4600 m above sea level (a.s.l.). It originates from the Jima Yangzong glacier at 5200 m a.s.l. in the northern Himalayas and flows eastwards along the Indus-Tsangpo suture with a relatively flat terrain. Subsequently, it flows southwestwards with a sharp drop in elevation near Namche Barwa, then into India (where it is called the Brahmaputra River) and eventually into the Bay of Bengal. The climate and geological setting of the study area are described by Zhang et al. (2021a) and briefly described here.

The climate of the YTR catchment is significantly affected by topography, the Indian monsoon and westerly winds; thus it is subject to obvious spatial and seasonal differences. The climate in the upper reaches is cold and arid, whereas that in the lower reaches is relatively warm and wet. In the upper reaches, glacier/snow melt water and groundwater (e.g. springs) mostly recharge the river water, and in the middle and lower reaches precipitation is the main source. The recharge is affected by increased precipitation and glacier/snow melt water in summer and increase significantly during the July to August monsoon, when it is several times greater than during the non-monsoon season. Moreover, turbid river water is observed during the monsoon (Fig. S1) possibly owing the large amount of weathered products, soils, and sediments washed into the river water during that period. Geologically, the YTR basin extends approximately eastwards along the collisional suture zone of the Indian and Eurasian tectonic plates. Due to the east-west extension of the TP, several north-south rifts (the Dingri-Nima, Dingjie-Xietongmen-Shenzha, Yadong-Dangxiong-Gulu, and Gudui-Sangri rifts) cut across the YTR basin (Armijo et al., 1986). In the rift zones, geothermal fields (e.g. Yangbajain) commonly occur and geothermal water in the form of hot springs is discharged into the water of the YTR. Herein, direct input from hot springs has been observed into the YTR mainstream in the Semi geothermal field (Fig. S2).

3. Materials and methods

3.1. Sampling and field measurement

Samples of silicate rock (e.g., granites), aeolian deposits (sand dune) and hot spring water were collected from the YTR basin in June 2017 and July 2021 to investigate the potential source of dissolved Li in the catchment. Dissolved and SPM samples from mainstream and major tributaries were collected in June 2017 (before-monsoon, BM) and September 2017 (after-monsoon, AM) and monthly dissolved samples from four fixed sampling sites were collected from October 2017 to September 2018 to investigate the possible influences on the spatiotemporal δ^7Li_{dis} variation

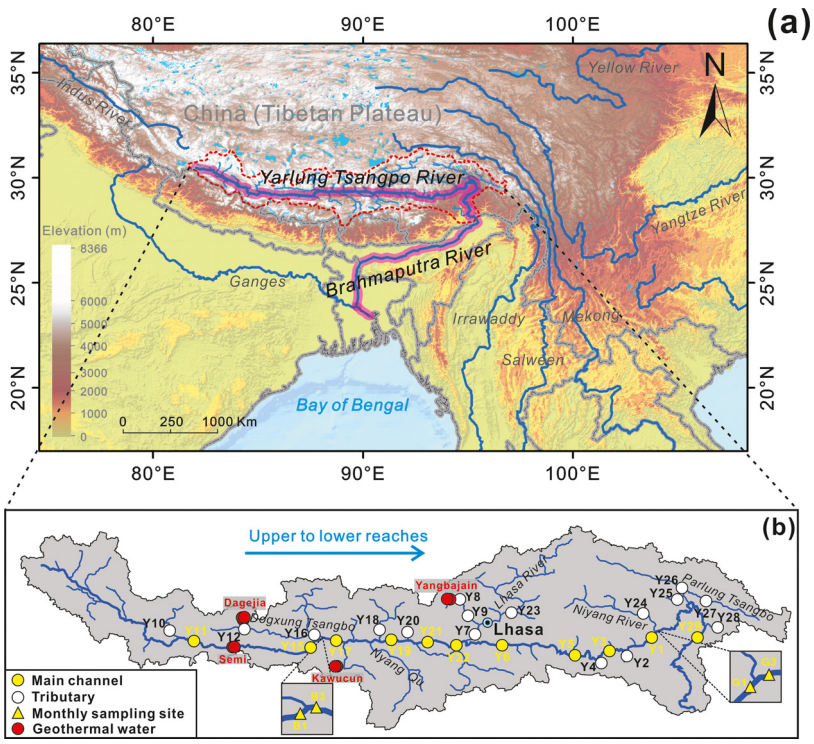

Fig. 1. Sampling sites in the Yarlung Tsangpo River (YTR) system. (For interpretation of the colors in the figure(s), the reader is referred to the web version of this article.)

(Fig. 1). In addition, geothermal waters, river sediments, and SPM samples were collected in July 2021 for use in adsorption experiments. More detailed river water sampling information can be found in Zhang et al. (2021a).

The temperature and pH of each water sample were measured in situ using a multi-parameter portable meter (MultiLine® IDS 3430, WTW). The pH electrode was pre-calibrated with buffers before measurement. Alkalinity was determined using the Gran titration method within 24 h of sampling. Each water sample was obtained using a peristaltic pump and filtered through a 0.45 μm cellulose membrane in the field. Each SPM sample was rinsed from the filter membrane using ultra-pure water and collected in a pre-cleaned centrifuge tube. The water samples for analyses of major cations and trace elements were stored in acid-washed 120 mL high-density polyethylene bottles and acidified with double-distilled HNO_3 to pH < 2. For anion analysis, water samples were stored in ultra-pure water pre-cleaned 15 mL centrifuge tubes without acidification. For Li isotope analysis, water samples were collected in acid-washed 1.5 L polyethylene bottles and acidified with 1 mL of double-distilled HNO_3. All the samples were stored at 4 °C until laboratory analysis.

3.2. Adsorption experiment

The adsorption experiment has been performed to assess Li isotope fractionation during geothermal water dissolved Li adsorption on the secondary minerals of SPM and river sediment. A filtered hot spring sample H9 without acidification was diluted with ultra-pure water to approximately 132 μg/L Li concentration. Three SPM samples with wet weights of 3.0, 6.8 and 6.2 g and one 15.0 g river sediment sample were placed in four 150 mL Erlenmeyer flasks. Afterword, 50 mL of diluted hot spring water sample was added to each flask. The flasks were placed on a shaker at 180 rpm at 20 °C for 7 days. Lastly, centrifugation and subsequent filtration through a 0.45 μm cellulose membrane were performed. The water sample was retained and acidified for elemental and Li isotope analyses.

3.3. Analytical methods

Major cation and anion concentrations in the water samples were analyzed via ICP-OES (Varian Vista-MPX) and ion chromatography (Dionex ICS-90), respectively. The solid samples (rocks, SPM, river sediments and aeolian deposits) were homogenized and ground in an agate mill (<200 mesh) for elemental and Li isotope analyses. The SPM and river sediment samples were freeze dried at −40 °C before grinding. The major element contents of the solid samples were analyzed by X-ray fluorescence (Shimadzu XRF-1800). Trace element concentrations in the water and solid samples after acid digestion were determined using an ICP-MS (PerkinElmer NexION 300X). Two Chinese national standard samples GBW07103 (granite) and GBW07105 (basalt) were used to calibrate the instrument for solid major element determination. The U.S. Geological Survey rock standards BCR-2 and GSP-2 were adopted to evaluate the accuracy of the major and trace elemental analyses. Precision for most major and trace elements in both water and solid samples was better than ± 5% (2σ) and ± 10% (2σ), respectively. Most analyses were conducted at the State Key Laboratory of Environmental Geochemistry, Institute of Geochemistry, Chinese Academy of Sciences.

Li isotope analysis was described in detail in our recent study (Zhang et al., 2021b). Each water sample containing about 400 ng of Li was transferred into a Teflon beaker and dried on a hot plate at 120 °C, followed by successive refluxing with 1 mL of distilled HNO_3 and 1 mL of distilled HCl. The final dried sample was then re-dissolved in 1 mL of 0.40 M HCl for column separation. For the solid samples, about 50 mg of powder was dissolved in a 4 mL mixture of distilled HF and HNO_3 (3:1, vol/vol) contained in a 7 mL Savillex™ screw-top beaker, subsequently dried on a hot plate for 48 h at 120 °C, followed by successive refluxing with 1 mL of distilled HNO_3 and 1 mL of distilled HCl, and re-dissolved in 1 mL of 0.40 M HCl for column separation. Li was purified using a cation exchange column loaded with resin (Bio-Rad™ AG 50 W-X12, 200-400 mesh) and eluted with 0.40 M HCl. The purification steps for the solid samples were duplicated to ensure complete Li

separation from its matrices. The eluents also collected before and after the Li-contained samples were determined to ensure full Li recovery. The Li-containing samples were dried and re-dissolved in 2% HNO_3 for multi-collector ICP-MS (Thermo Scientific™ Neptune Plus) analysis. Standard-sample bracketing with the L-SVEC standard (NIST RM 8545) was used herein. The Li concentrations in the samples and standard were both about 80 ng/mL. The external precision (2σ) using this technique was better than ± 0.7‰ obtained by the repeated dissolution, purification, and determination of seawater and rock standards. The measured δ^7Li values of a seawater sample and rock reference materials of AGV-2 and GSP-2 were +31.2 ± 0.7‰ ($n = 8$), +7.1 ± 0.5‰ ($n = 3$), and −0.12 ± 0.4‰ ($n = 4$), respectively, all of which are consistent with previous works (e.g., Liu et al., 2015).

4. Results

The major element and Li concentrations and Li isotope compositions of all of the samples in this study are listed in Tables S1-S5.

4.1. Major elements in geothermal water and river water

The geothermal waters are enriched in $[Na]_{dis}$ (286–780 mg/L) and $[Cl]_{dis}$ (157–621 mg/L) (Table S1), which is in agreement with the published data for other geothermal waters in the TP (e.g., Ma et al., 2020). The $[Na]_{dis}$ and $[Cl]_{dis}$ in river water are in the ranges of 0.5–21.6 mg/L (mean 8.3 mg/L, $n = 97$) and 0.1–14.8 mg/L (mean 4.5 mg/L, $n = 97$), respectively (Tables S2 and S3). These high values are observed in the mainstream and upstream tributaries (Fig. S3).

4.2. Li/Na molar ratios

The Li/Na (×1000) molar ratio in the mainstream and upstream tributaries varies between 9.9 and 62 (mean 22, $n = 78$) (except for G3-5). These values are higher than reported for most other rivers in the world (Weynell et al., 2021). Sample Y9 obtained from a stream near the Yangbajain geothermal field in June 2017 has the highest Li/Na ratio (~62). Interestingly, the Li/Na values of river waters are significantly higher than those of silicate rocks in the TP (e.g., granites (1.2–1.9) (this study); basalts (2.0–5.8) (Ma et al., 2020), aeolian deposits in the study area (~4.9) and the average upper continental crust (~4.1) (Rudnick and Gao, 2003)). However, most Li/Na values are much lower than those of the geothermal water (53−154, n = 9) herein.

4.3. Lithium concentration and isotope ratios

4.3.1. Solid samples

The solid sample data in Table S4 show variation in the [Li] and δ^7Li values of the granite samples between 10.3 and 16.5 mg/kg and between +1.2 and +3.7‰, respectively. They are close to the statistical means reported by Teng et al. (2009) for worldwide granites (33 ± 32 mg/kg (1σ), 2.0 ± 2.3‰ (1σ)). The [Li] and δ^7Li values of the aeolian deposition sample are 29.2 mg/kg and +0.7‰, similar to 30.5 ± 3.6 mg/kg and +0.6 ± 0.6‰ in the upper continental crust (Sauzéat et al., 2015), respectively.

4.3.2. Geothermal water

Extremely high $[Li]_{dis}$ occurs in geothermal waters (5.5–34.4 mg/L, mean 15.7 mg/L, $n = 9$) (Table S1). The δ^7Li_{dis} is low and varied within a narrow range of −1.7‰–+3.1‰ (mean +1.0‰). High levels of $[Li]_{dis}$ with relatively low δ^7Li_{dis} have also been reported for other TP geothermal waters (Weynell et al., 2017; Ma et al., 2020), as well as in geothermal fields worldwide (Fig. 2).

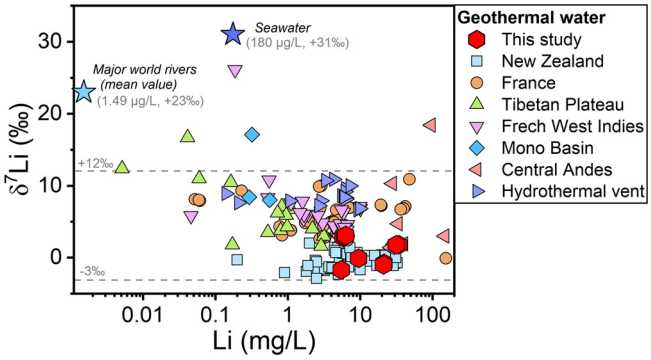

Fig. 2. Dissolved Li concentration versus of geothermal water in the YTR basin (this study), New Zealand (Millot et al., 2012; Bernal et al., 2014), France (Millot and Négrel, 2007), Tibetan Plateau (Weynell et al., 2017; Ma et al., 2020), French West Indies (Millot et al., 2010), Mono Basin (Tomascak et al., 2003), Central Andes (Godfrey et al., 2013), and Hydrothermal vent (Chan et al., 1993; Foustoukos et al., 2004). Statistical mean values of Li concentration and δ^7Li for these geothermal waters are +3.9 ± 4.1‰ (1σ) and 9.5 ± 17.5 mg/L (1σ) (n = 211), respectively. Seawater and the mean major world river data are from Misra and Froelich (2012) and Huh et al. (1998), respectively.

4.3.3. Dissolved load in river water

The $[Li]_{dis}$ varies greatly (0.5–313 μg/L, Tables S2 and S3), with a mean concentration of 58.4 μg/L ($n = 93$), which is about 30 times the worldwide riverine average (1.49 μg/L). Similar to the $[Na]_{dis}$ and $[Cl]_{dis}$ in river water, the high $[Li]_{dis}$ values are mainly distributed in the mainstream and upstream tributaries (Fig. S3). Spatially, the $[Li]_{dis}$ in the mainstream and tributaries shows a decreasing trend towards downstream for both BM and AM samples (Fig. 3). Seasonally, in most cases, the $[Li]_{dis}$ in river water from the same sampling sites before-monsoon is higher than that after-monsoon (Table S2). The $[Li]_{dis}$ varies significantly at the fixed sampling sites in each month of a hydrological year. For example, $[Li]_{dis}$ values vary between 22.5 and 139 μg/L at site B1 from October 2017 to September 2018. Moreover, the lower $[Li]_{dis}$ values are generally observed during the monsoon season (July and August) (Fig. 4).

The δ^7Li_{dis} values range from +1.0‰ to +14.7‰ (mean +6.4‰, $n = 92$), except for the downstream sample Y25 (Table S2). These values are much lower than most worldwide published riverine δ^7Li_{dis} data, including the mean value of +23.5‰ (Huh et al., 1998). The lowest δ^7Li_{dis} (+1.0‰) has been observed in sample Y9 from a stream close to the Yangbajain geothermal field collected in June 2017. The mainstream δ^7Li_{dis} value is stable throughout the river flow before-monsoon season (+3.1‰ to +4.8‰). It gradually increases from +3.1‰ to +7.6‰ towards the downstream after-monsoon season (Fig. 3). Monthly data show that the mainstream δ^7Li_{dis} increases significantly during the monsoon season (July and August) in the range of +8.3‰ to +11.5‰, while relatively low values are observed in non-monsoon (+3.7‰ to +7.4‰), except for sample G3-5 (Fig. 4).

4.3.4. Suspended load in river water

Before-monsoon, the mainstream SPM concentrations vary between 2.3 and 11.5 mg/L, except for sample Y29 from the site farthest downstream herein. After-monsoon, the values increase to 3.2–339 mg/L (mean 102 mg/L, $n = 23$) and tend to increase from upstream to downstream. SPM samples were not collected for monthly sampling in this study; the three-yearly average monthly SPM concentration in the mainstream was compiled by Shi et al. (2018). Suspended Li concentrations ($[Li]_{sus}$) of 43–168 mg/kg (mean 82 mg/kg, $n = 42$) are much higher than those of the granite and aeolian deposition samples (see above, Table S4). The δ^7Li_{sus} values vary from −8.9‰ to −0.6‰ (mean −4.6‰, n = 38), which is much lower than the δ^7Li_{dis} in river waters and geother-

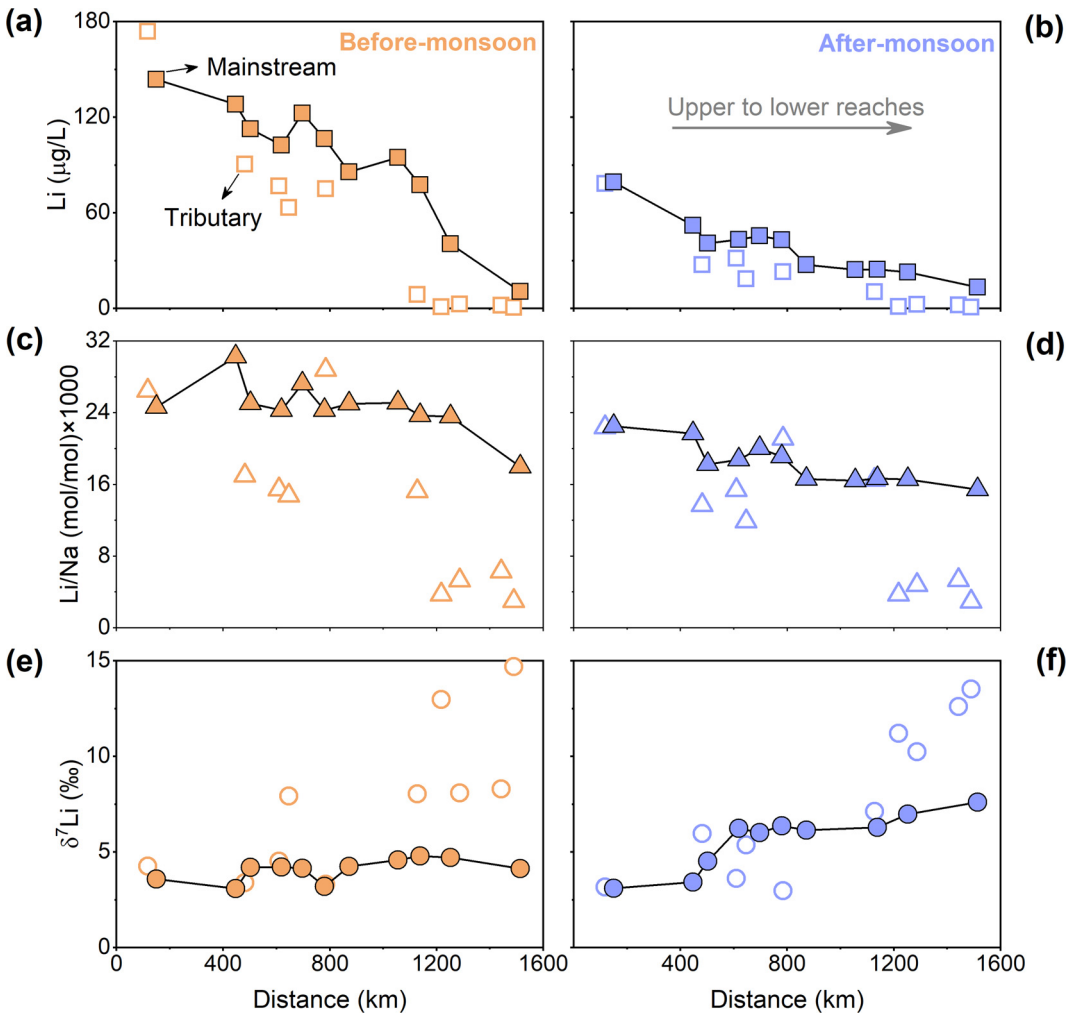

Fig. 3. Dissolved Li concentration, δ^7Li_{dis} value, and molar ratio of Li/Na (×1000) versus the river flow distance of the YTR. The filled and open symbols represent mainstream and tributary of the YTR, respectively. The orange and blue symbols represent the river water samples collected before- (June 2017) and after- (September 2017) monsoon seasons, respectively.

mal waters in the catchment. These data are consistent with the previously reported indication that the Li isotope composition of SPM is generally lighter than that of dissolved load in river water (e.g., Kısakürek et al., 2005; Pogge von Strandmann et al., 2006; Dellinger et al., 2015; Wang et al., 2015).

4.3.5. Adsorption experiments

Adsorption experiment results are listed in Table S4. The final experimental $[Li]_{dis}$ values vary between 27.6 and 35.1 μg/L, which are significantly lower than in the initial solution (132 μg/L). Between 73% and 79% of dissolved Li in geothermal water was removed by the YTR SPM or river sediment. The final experimental δ^7Li_{dis} values (+10.4‰–+18.0‰) are significantly higher than the initial value of +3.1‰ (Fig. 5).

5. Discussion

5.1. Geothermal water inputs cause high levels of dissolved Li in the Yarlung Tsangpo River

Dissolved Li in most rivers is predominantly sourced from silicate weathering, even in carbonate-dominated catchments (e.g., Kısakürek et al., 2005). However, it does not explain the high $[Li]_{dis}$ in the YTR. This is mainly because Li is less conservative than Na and is preferentially retained in the solid phase during weathering, whereas the dissolved Li/Na ratios in most of the river water samples are found to be significantly higher than that of silicate rocks in the TP. These findings suggest that much of the dissolved Li in the river water may come from a different source with a relatively high Li/Na ratio. Generally, shale has a high Li content and high Li/Na ratio (Teng et al., 2004), making it a potential end member for high $[Li]_{dis}$ and Li/Na ratio in river water. Unexpectedly, a study from Shale Hills (Appalachian Mountains, USA) showed low $[Li]_{dis}$ (<1 μg/L) in stream waters draining from the shale weathering area (Steinhoefel et al., 2021), which does not support the fact that the high $[Li]_{dis}$ observed herein comes from shale weathering. Some studies have suggested that evaporite dissolution is the major cause of high $[Li]_{dis}$ in the Jinsha River (headwaters of the Yangtze River) from the eastern TP (Wang et al., 2015; Ma et al., 2020). However, the reported Li/Na ratios in evaporites (1.7–2.7) are significantly lower than that in the YTR waters (Wang et al., 2015). Additionally, we rarely find any evaporite deposits in the YTR basin. This is consistent with the results from Weynell et al. (2021), where evaporite dissolution contributes little (<7.5%) to the dissolved Li in the YTR. Anthropogenic activity may cause elevated $[Li]_{dis}$ in river water (Choi et al., 2019), but the impact on the YTR catchment should not be significant because of the low population density in the TP. Lastly, atmospheric precipitation and glacier melt from the TP generally contain low $[Li]_{dis}$ (Ma et al., 2020); hence, these are not likely responsible for the high levels of

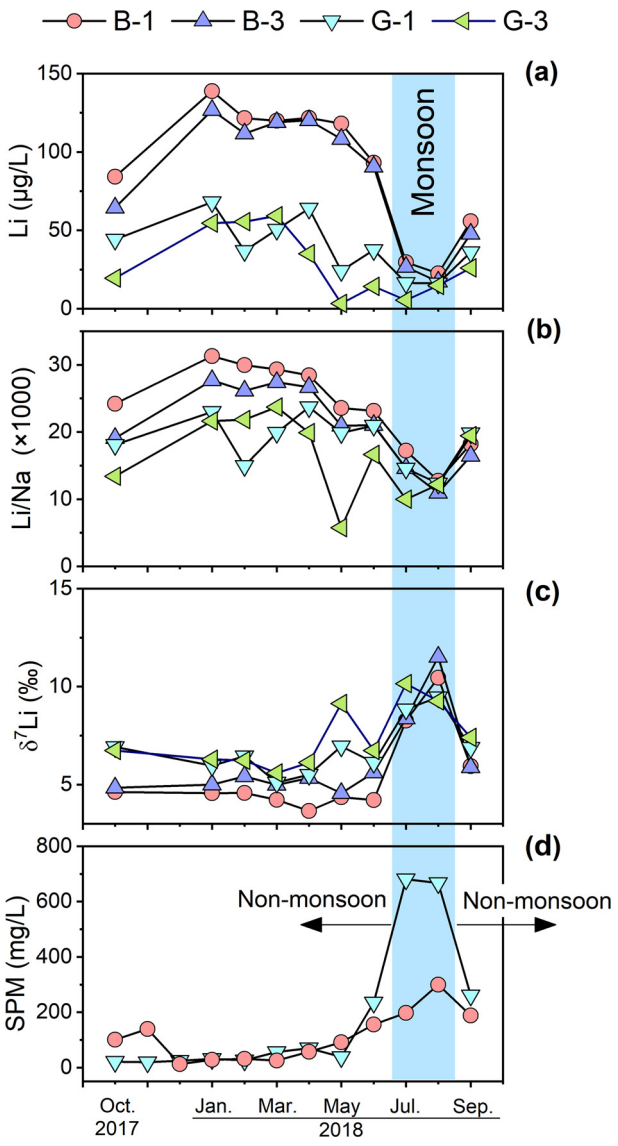

Fig. 4. Monthly variations of dissolved Li concentration, δ^7Li_{dis} value, molar ratio of Li/Na (×1000), and SPM concentration in river waters of the YTR. The locations of these fixed sampling sites are present in Fig. 1. Data of the SPM concentration are three-year average for the mainstream from 2007 to 2009 and are from Shi et al. (2018).

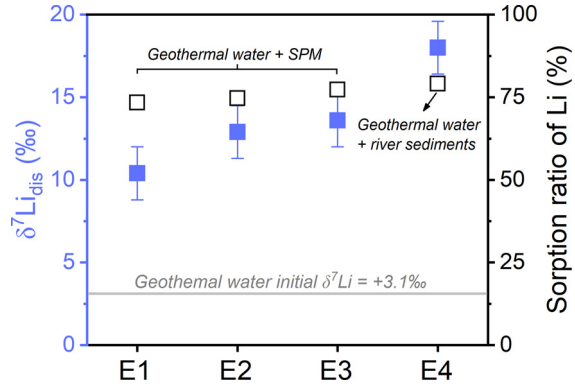

Fig. 5. The δ^7Li_{dis} value and sorption ratio of Li for the adsorption experiment. The samples E1, E2, and E3 are "Geothermal water + SPM" and the sample E4 is "Geothermal water + river sediment". The grey line is the δ^7Li value (+3.1‰) in the initial geothermal water sample H9. The blue and black squares represent the δ^7Li value and sorption ratio of Li in final experimental solutions.

dissolved Li in the YTR (see details in the Supplementary Information).

Geothermal water is likely to be the main source of high $[Li]_{dis}$ in the studied river waters. The main evidence is from the high $[Li]_{dis}$ (at the mg/L level) observed in the geothermal water of the basin (Table S1). In addition, Li et al. (2022) have shown that the extremely high $[Li]_{dis}$ in geothermal waters in the southern TP is mainly sourced from semi-molten state magma degassing rather than leaching from the surrounding rocks; thus, the Li/Na ratio of geothermal water is significantly higher than that of silicate rocks in the study area. The high Li/Na ratio in the geothermal water explains the observed high Li/Na ratios in the river waters. Affected by the input of geothermal water, the $[Li]_{dis}$ is as high as 313 μg/L (sample Y8, June 2017) in the Duilong Qu tributary which flows through the Yangbajain geothermal field. The $[Li]_{dis}$ in river water is far lower than that in geothermal water as it is diluted by atmospheric precipitation or glacier melt. The conservative element Cl is also enriched in geothermal water, which reflects the dilution process. The data points of $[Li]_{dis}$ vs. $[Cl]_{dis}$ in river water are almost all distributed near the theoretical (or conservative) dilution lines of geothermal water, except for the low $[Li]_{dis}$ content of tributaries from the lower reaches (Fig. 6). This further confirms that geothermal water is the predominant source of high levels of dissolved Li in the YTR. More importantly, our quantitative calculations show that the contribution of dissolved Li from geothermal water is >85% (mean 91%, $n = 79$) in most samples, except in the tributaries in the lower reaches (detailed calculations in the Supplementary Information).

5.2. Factors affecting the dissolved Li isotope composition in the Yarlung Tsangpo River

5.2.1. Mixing between geothermal water and silicate weathering

Since most dissolved Li in the YTR is derived from geothermal water, the dissolved Li isotope composition in river water largely inherits the isotopic signature of geothermal water, which has very low δ^7Li_{dis} values (−1.7‰–+3.1‰). This agrees well with the low δ^7Li_{dis} values observed in most of the river water samples, which are mainly distributed in the middle and upper reaches where abundant geothermal fields are present. The lowest δ^7Li_{dis} (+1.0‰) value is in sample Y9 from the river flowing through the Yangbajain geothermal field for which geothermal samples H1 and H2 have δ^7Li values of −0.1‰ and −1.7‰, respectively (Table S1).

Although the geothermal water inputs explain the low δ^7Li_{dis} values in the YTR, the river water has higher δ^7Li_{dis} than that of the geothermal water. It has been shown that some other rivers in the TP were less affected by geothermal water input (e.g., Kısakürek et al., 2005; Bohlin and Bickle, 2019). The dissolved Li in those rivers is mainly sourced from silicate weathering, which yields higher δ^7Li_{dis} values (mean +17.9‰, $n = 62$) than that of the geothermal water (Fig. 7). In this study, most of the tributaries in the lower reaches have higher δ^7Li_{dis} values (up to +20.3‰) (Table S2), which does not seem to be affected by geothermal water. This is mainly due to the fractionation of Li isotopes during Li incorporation into clay minerals formed by silicate weathering, yielding an elevated δ^7Li_{dis} in river water. Therefore, because other sources of Li contribute little to dissolved Li in the YTR, the ratio of dissolved Li from geothermal water (low δ^7Li_{dis}) and silicate weathering (high δ^7Li_{dis}) may control the variation of δ^7Li_{dis} in the river water.

A mixing model is used to further evaluate the contribution between the two end members to the dissolved Li isotope composition in river water. Herein, a conservative mixing of dissolved Li from geothermal water and silicate weathering in the river water is assumed. Interestingly, almost all of the data points (δ^7Li_{dis} vs. Li/Na) do not fall near the theoretical mixing line between

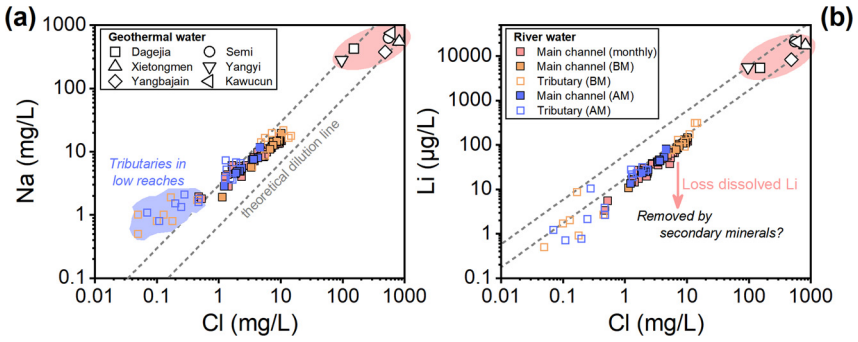

Fig. 6. The relationships between Na and Cl, Li and Cl concentrations in river water and geothermal water from the YTR basin. Data of geothermal water is the statistical mean values of the hot springs in each geothermal field. Data for Xietongmen and Yangyi geothermal fields are from Zhang et al. (2021a). The theoretical dilution lines are based on the assumption that the element concentrations of geothermal water input rivers are only affected by dilution process.

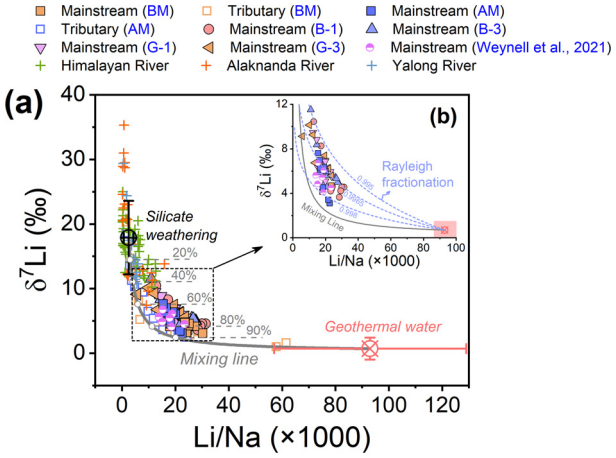

Fig. 7. Dissolved Li/Na molar ratios (×1000) plotted against δ^7Li value for river water and geothermal water from the YTR and some other rivers in the Tibetan Plateau. The "BM" and "AM" refer to before- and after-monsoon, respectively. The solid grey line is the theoretical binary mixing results of dissolved Li from silicate weathering and geothermal water. Silicate weathering δ^7Li value (+17.9 ± 5.7‰ (1σ), n = 62) and Li/Na ratio (2.5 ± 1.8 (1σ), n = 62) are statistical means of lower reaches tributary in YTR (this study), Himalayan River (Kısakürek et al., 2005), Alaknanda River (Bohlin and Bickle, 2019), and Yalong River (Ma et al., 2020), which are hardly affected by geothermal water. River samples with a Li/Na ratio greater than 6.0 were not used due to it may be contaminated by geothermal water (see Fig. 8). Geothermal water δ^7Li value (+0.7 ± 1.7‰ (1σ), n = 4) and Li/Na ratio (93 ± 36 (1σ), n = 4) is the statistical means of the four geothermal field in this study (Table S1). The blue dashed lines are Rayleigh fractionation relationships and using the geothermal water as the initial δ^7Li value and Li/Na ratio (see text for details). Results of theoretical binary mixing and Rayleigh fraction for extremum values (±1σ) of δ^7Li and Li/Na of the two end members are shown in Figure S5.

geothermal water and silicate weathering, but appear above the line (Fig. 7). In addition, the tributaries in the lower reaches have relatively high δ^7Li_{dis} values, but their influx does not change the δ^7Li_{dis} values in the mainstream (BM) (Fig. 3). This is mainly because the $[Li]_{dis}$ in these tributaries is low and does not significantly affect the Li flux and its isotopic composition in the mainstream. These results suggest that the variations of δ^7Li_{dis} in the YTR cannot be simply explained by the mixing of dissolved Li between geothermal water and silicate weathering.

5.2.2. Ongoing Li isotope fractionation between dissolved Li and secondary minerals in river water

Experiments have shown that Li isotope fractionation during Li partition between solid and liquid phases is mainly due to the fact that light ^{6}Li tends to be incorporated into (or adsorbed onto) secondary minerals (e.g. clays), affording the preferential enrichment of heavy ^{7}Li in the liquid phase (e.g., Zhang et al., 1998; Kısakürek et al., 2005; Pogge von Strandmann et al., 2006; Vigier et al., 2008; Dellinger et al., 2015; Wang et al., 2015; Li and Liu, 2020). Generally, most clay minerals in SPM and bed sediments in rivers originate from the chemical weathering of silicate rocks. Previous work has shown that the bed sediments from the YTR contain a high proportion of clay minerals such as kaolinite, illite, and chlorite (He et al., 2013). Consequently, once geothermal Li has entered the river water, dissolved Li may be further fractionated during its incorporation into (or adsorbed onto) the SPM or bed sediments. This speculation is supported by the observation that the SPM has a high Li content but low δ^7Li_{dis} (from −8.9‰ to −0.6‰) compare to geothermal water (Table S1). Because more ^{6}Li enters the SPM, the dissolved load in the river water is relatively rich in ^{7}Li and shows a higher δ^7Li_{dis} than that of geothermal water. Moreover, the δ^7Li_{dis} increase with decreasing Li/Na ratio in river water (Fig. 7) confirms that some of the dissolved Li is removed by SPM, and ^{6}Li preferentially enters the solid phase (Liu et al., 2015). The adsorption experiment results here suggest that significant Li isotope fractionation occurs during the geothermal dissolved Li incorporation into the SPM or bed sediments and final δ^7Li_{dis} increases from 7.3‰ to 14.9‰ (Fig. 5), further confirming that ongoing Li isotope fractionation occurs as geothermal Li is transported in river water. This view is consistent with the adsorption experiment results by Zhang et al. (1998), who found that obvious Li isotope fractionation during dissolved Li was removed by the Mississippi River SPM. Importantly, several field studies have also suggested that ongoing isotopic fractionation when Li is being incorporated into SPM considerably contributes to the δ^7Li_{dis} increase in river water (e.g., Kısakürek et al., 2005; Pogge von Strandmann et al., 2006; Wanner et al., 2014; Dellinger et al., 2015; Liu et al., 2015; Ma et al., 2020).

The spatiotemporal variation of δ^7Li_{dis} also supports that ongoing Li isotope fractionation occurs in waters of the YTR. The SPM concentration positively correlates with the δ^7Li_{dis} in the river mainstream (Fig. S4), likely indicating that more SPM preferentially scavenges more ^{6}Li from the dissolved load. Monthly data also show that the δ^7Li_{dis} value co-varies with SPM concentration in the mainstream with both peaking the monsoon season (Fig. 4). This is consistent with a previous study by Wanner et al. (2014), who suggested that SPM concentration plays an important role in regulating the variation of δ^7Li_{dis} in river water, and that δ^7Li_{dis} increases as the SPM concentration increases. This view seems inconsistent with the results from the Yellow River that the seasonal changes in δ^7Li_{dis} were not correlated with the SPM concentration. Gou et al. (2019) speculated that the saturation of Li in SPM (or loess surface) is the major cause of the discrepancy. In the TP, there are more exposed fresh rocks that produced a large amount of newly formed secondary minerals, which are washed into river water during the monsoon, supplying additional fresh clay and/or oxyhydroxide minerals with more cavity lattices or adsorption sites for Li isotope fractionation. This speculation is supported by a recent study that the rapidly forming secondary

mineral (e.g., poorly-crystalline allophane) dominates Li isotope fractionation over more slowly-forming crystalline clays (Pogge von Strandmann et al., 2021).

Rayleigh fractionation (Eq. (1)) and batch fractionation (Eq. (2)) are commonly used to quantify Li isotope fractionation during weathering, calculating the fractionation factor (α) between solid and dissolved loads (e.g., Li) during water-rock interactions. The model equations are described well in some works (e.g., Bagard et al., 2015), and are shown as follows:

$$\delta^7Li_{dis} = \delta^7Li_0 + (\alpha_{sec\text{-}dis} - 1) \times \ln(f_{Li}) \times 1000 \quad (1)$$

$$\delta^7Li_{dis} = \delta^7Li_0 + (\alpha_{sec\text{-}dis} - 1) \times (1 - f_{Li}) \times 1000 \quad (2)$$

$$f_{Li} = (Li/Na)_{dis}/(Li/Na)_0 \quad (3)$$

where δ^7Li_0 and $(Li/Na)_0$ are the initial values corresponding to the mean values of regional silicate rocks or the upper continental crust, and $\alpha_{sec\text{-}dis}$ is the Li isotope fractionation factor between secondary weathering products and the dissolved load.

The dissolved Li is mainly derived from geothermal water in the study catchment (except for the tributaries in the lower reaches); therefore, the geothermal water δ^7Li and Li/Na ratio as the initial values are used to model the isotopic fractionation during Li transport in river water. Most of the data points fall on the Rayleigh fractionation curves rather than the batch fractionation curve using α values of 0.995–0.998 (Fig. 7), which is consistent with the continuous isotopic fractionation calculated by Rayleigh fractionation (Maffre et al., 2020). This range of α is comparable to those of other rivers originating in the Himalayas, such as the Brahmaputra (low reaches), Ganges, and Yangtze River (headwaters) (Bagard et al., 2015; Pogge von Strandmann et al., 2017; Ma et al., 2020; Yoshimura et al., 2021). The variation in α is likely related to the assemblage of the secondary minerals of the weathering products in rivers (e.g., Ma et al., 2020), because a large variation of α values (0.971–1.000) for different secondary minerals has been determined experimentally (Penniston-Dorland et al., 2017; Pogge von Strandmann et al., 2020; Li and Liu, 2022). However, recent experimental and field studies have suggested that the fractionation factor imposed by Li incorporation into secondary minerals is fairly constant, and not dependent on mineralogy (Hindshaw et al., 2019b; Pogge von Strandmann et al., 2021, 2022). Moreover, the amount of newly formed clay minerals is the key process in controlling the degree of Li isotope fractionation during silicate weathering (Pogge von Strandmann et al., 2021). Meanwhile, because the $(Li/Na)_0$ ratio is a basic parameter for calculating the α value (Eqs. (1) and (3)), the difference in the $(Li/Na)_0$ ratio changes the Li isotope fractionation factor. For instance, the regional mixed type of silicate rock and the uptake/desorption of Na into/from some secondary minerals (e.g. zeolites) may cause a change in the $(Li/Na)_0$ ratio and are an important reason for the variation of α values in a catchment (Pogge von Strandmann et al., 2017; Murphy et al., 2019). Herein, the geothermal water Li isotope composition has relatively stable initial values (i.e., δ^7Li_0), but the $(Li/Na)_0$ ratio shows a wide range of variations in different geothermal fields (Table S1). This may be the main reason for the variation of the calculated α values in the YTR.

5.2.3. Other potential factors

Other potential factors can also contribute to the observed δ^7Li_{dis} herein. For example, previous studies have suggested that temperature may be an important influencing factor in seasonal variations in dissolved Li isotope composition, where they showed that temperature was negatively correlated with δ^7Li_{dis} in river water (Gou et al., 2019). However, this view does not explain the finding of the present study that temperature is positively correlated with δ^7Li_{dis} (Fig. S6). In addition, dilution by rainwater with high δ^7Li_{dis} values may considerably increase the riverine δ^7Li values, especially during the monsoon. However, the calculated results suggest that precipitation has a negligible effect on the variation in δ^7Li_{dis} (see details in the Supplementary Information). Moreover, the changes in the contribution of shallow groundwater with Li isotope composition different from river water may cause variations in δ^7Li_{dis} in river water in different seasons (Liu et al., 2015; Manaka et al., 2017; Hindshaw et al., 2019a). Herein, we assume that the dissolution of soil evaporites and/or groundwater (or other sources) input more Li with high δ^7Li_{dis} values during the monsoon season, causing an increase in the riverine δ^7Li_{dis}. Afterwards, dissolved Li flux in the river might increase significantly during this period. However, the Li_{dis} flux monthly variation does not seem to support this assumption, especially because the δ^7Li_{dis} value exhibits opposite rhythms to the Li_{dis} flux at site G3 from March to September 2018 (Fig. S7). The observation that a higher δ^7Li_{dis} value corresponds to a lower Li_{dis} flux may be due to the incorporation of more Li into secondary minerals and the resulting continued fractionation of Li isotopes. Alternatively, soil evaporites (or soil water) may enrich heavy ^7Li during the evaporation process (Xu et al., 2021). The YTR has an arid climate and strong evaporation, especially in the middle and upper reaches. As a result, Li in soil evaporites may be washed into the YTR by rainfall runoff; this may also contribute to the increase in δ^7Li_{dis} in river water during the monsoon season. This process has been confirmed in a study of the seasonal changes of δ^7Li_{dis} in the Yellow River (Gou et al., 2019).

5.3. Implications for the relationship between the tectonic uplift and increase in seawater δ^7Li value

The variation of the seawater δ^7Li over the Cenozoic is controlled by changes in continental weathering associated with tectonic uplift. For example, Misra and Froelich (2012) suggested that the tectonic uplift of the Himalayas shifted the continental weathering regime from congruent weathering in the early Cenozoic to more incongruent weathering in the Late Cenozoic. After incongruent continental weathering occurring in floodplains had formed more secondary minerals and fractionation of Li isotopes in river systems, the δ^7Li_{dis} values in river estuaries increased and raised these values in the oceans (Pogge von Strandmann and Henderson, 2015). Other factors, such as climate cooling and changes in aridity, may also have contributed to the rise in river δ^7Li values and, in turn, influenced the marine Li isotope composition (Gou et al., 2019; Xu et al., 2021). Alternatively, other scenarios can explain the increase in seawater δ^7Li value. For example, Vigier and Goddéris (2015) suggested that the river δ^7Li_{dis} remained stable; however, increasing the continental dissolved Li flux to the ocean could explain the Cenozoic δ^7Li rise. Moreover, increased physical erosion following mountain uplift may have caused more degraded continental materials to be delivered into the oceans, which can increase seawater δ^7Li in two ways. First, eroded materials continuously react with river water and further increase dissolved δ^7Li in rivers during riverine transportation, delivering high δ^7Li in the ocean (Wanner et al., 2014). Second, more degraded continental materials can increase the amount of marine sedimentary authigenic clays, which preferentially sequester the light Li into authigenic clays, producing increased δ^7Li in the ocean (Li and West, 2014). In summary, previous studies agree that there is a relationship between the tectonic uplift and variation of Li flux and isotopic composition in river water, but have mostly argued about the details of how tectonic uplift influences Cenozoic seawater δ^7Li.

Here, we notice that geothermal waters are often found in active tectonic areas and are rich in Li in the TP. The input of geothermal water significantly changes the Li flux and isotopic composi-

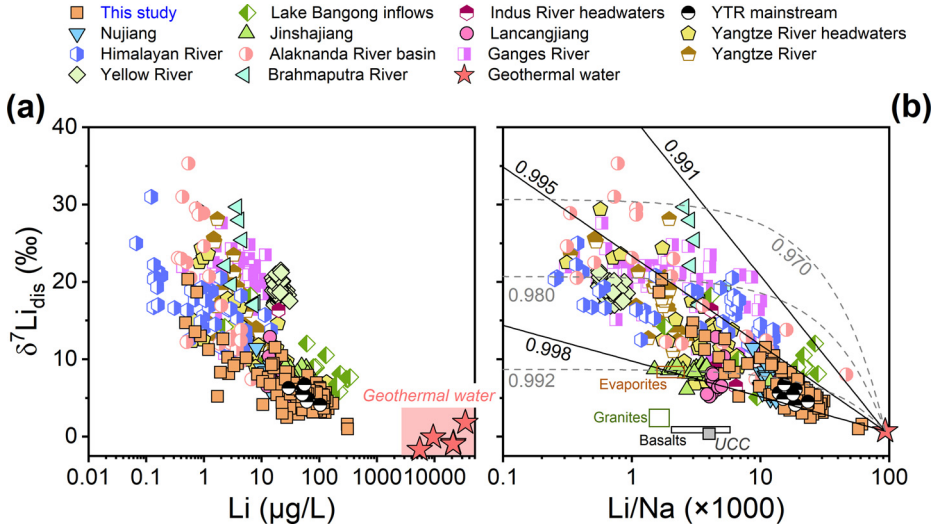

Fig. 8. The δ^7Li_{dis} value plotted against (a) dissolved Li concentration and (b) Li/Na molar ratio (×1000) for geothermal waters in the YTR basin and rivers originated from the Tibetan Plateau, including the YTR basin (this study), Lake Bangong inflows, Indus River headwaters, YTR mainstream (Weynell et al., 2021), Nujiang, Jinshajiang, Lancangjiang (Liu et al., 2011), Yangtze River headwaters (Ma et al., 2020), Himalayan River (Kısakürek et al., 2005), Alaknanda River basin (Bohlin and Bickle, 2019), Ganges River (Pogge von Strandmann et al., 2017), Yangtze River (Wang et al., 2015), Yellow River (Gou et al., 2019), Brahmaputra River (Bagard et al., 2015; Manaka et al., 2017). Some samples significantly affected by anthropogenic activities were not collected. The black solid lines and grey dashed lines are Rayleigh fractionation and Batch fractionation relationships, respectively, and using the geothermal water as the initial δ^7Li value and Li/Na ratio (Table S1). The black and grey numbers are fractionation factors for Rayleigh and Batch equations, respectively. The δ^7Li value and Li/Na ratios for granites in the Tibetan Plateau are from this study, while evaporite and basalt data in the TP are from Ma et al. (2020) and references therein, and the UCC values are from Rudnick and Gao (2003).

tion of river water in the areas. Since many large rivers originated from the TP, the geothermal water Li is partly transported by these rivers to eventually flow into the ocean. Submarine geothermal water is considered to have a relatively stable Li flux and isotopic composition, which has been directly input into the ocean since the Cenozoic (Misra and Froelich, 2012). Conversely, the dissolved Li in continental geothermal water does not directly feed into the ocean, but is transported by rivers over long distances and thus has long residence times. For the time that the dissolved Li is carried by rivers, more ^{6}Li is incorporated into the secondary minerals in the river as SPM or bed sediments, resulting in elevated riverine δ^7Li_{dis} by the time the river water eventually reaches the ocean. Studies on rivers originating in the TP suggest that much of the dissolved Li in the rivers is derived from geothermal water and Li isotope fractionation during dissolved Li removed from river water (Fig. 8).

Notably, the δ^7Li_{dis} value in the Ganges increased by about 10‰ for a relatively short flow distance from headwaters, while the value did not continue to increase and remained a constant of +21 ± 1.6‰ for a long flow distance in the floodplain (Pogge von Strandmann et al., 2017). This is mainly due to the fact that the Ganges floodplain is at a steady-state in terms of the primary mineral dissolution to secondary mineral formation ratio, referred to as 'weathering intensity' for most of its length. In more extreme cases, the dissolution of secondary minerals decreased the δ^7Li_{dis} in rivers from lowland with high weathering intensity in the Amazon River basin (Dellinger et al., 2015). The effect of the floodplain on the Li isotope composition in river water appears to be inconsistent in different regions (e.g., Dellinger et al., 2015; Pogge von Strandmann and Henderson, 2015; Wang et al., 2015; Pogge von Strandmann et al., 2017). The role of floodplains in controlling the δ^7Li_{dis} of large rivers needs to be deeply studied.

As discussed above, we found that the input of geothermal water Li induces a significant increase in riverine dissolved Li flux and δ^7Li_{dis} to the ocean, at least in the TP (Fig. 9). However, it is difficult to quantitatively assess the impact of this continental geothermal water on the global ocean Li budget and seawater δ^7Li. Since Li behaves non-conservatively and much of the dissolved Li is removed by secondary minerals during riverine transportation, the residual geothermal water Li flux ($Li_{flux\text{-}residual}$) in estuaries is lower than the initial total geothermal Li flux ($Li_{flux\text{-}total}$) in headwaters. It may be possible to estimate the $Li_{flux\text{-}residual}$ by Rayleigh fractionation (Eq. (1)) ($f_{Li} = (Li_{flux\text{-}residual})/(Li_{flux\text{-}total})$), assuming that the δ^7Li_{dis} is fixed at +23‰, and $\delta^7Li_0 = +1.0$‰ (geothermal water) and $\alpha = 0.995$ herein. Hence, if $Li_{flux\text{-}total}$ is known, then $Li_{flux\text{-}residual}$ can be calculated and the extent of the increase of seawater δ^7Li induced by geothermal water Li may be evaluated by the model suggested by Vigier and Goddéris (2015). Currently, few data are reported on the discharge of hot springs, making it difficult to calculate $Li_{flux\text{-}total}$. Future work requires more data on hot spring discharges and their Li concentrations to estimate $Li_{flux\text{-}total}$ and how these parameters change over the Cenozoic.

6. Conclusions

The YTR has very high concentrations of dissolved Li ($[Li]_{dis}$), high Li/Na ratios, and low δ^7Li_{dis} values, which cannot only be explained by the chemical weathering of silicates. Geothermal water with extremely high $[Li]_{dis}$ (at the mg/L levels) is probably responsible for high $[Li]_{dis}$ in river water. Although much of the dissolved Li in river water is derived from geothermal water, the dissolved Li isotope composition in the river water does not inherit the isotopic signature of the geothermal water. The mixing of dissolved Li sourced from geothermal water and silicate weathering cannot fully explain the spatiotemporal variation of δ^7Li_{dis} in the YTR. Ongoing Li isotope fractionation between dissolved loads and suspended materials occurs during riverine transportation. In addition, the model results show that this fractionation process follows Rayleigh fractionation. Geothermal activities occur in tectonic active areas and geothermal waters are rich in Li in the TP. Dissolved Li from continental geothermal water is transported by rivers over long distances; thus, they have long residence times, producing high riverine Li with elevated δ^7Li_{dis} discharging into the ocean. Hence, we speculate that tectonic uplift has afforded the formation of geothermal systems that provide most of the dissolved Li in river water and increase the riverine dissolved Li flux. In addition, the fractionation of Li isotopes occurs while the dissolved Li is transported by rivers over long distances with long residence

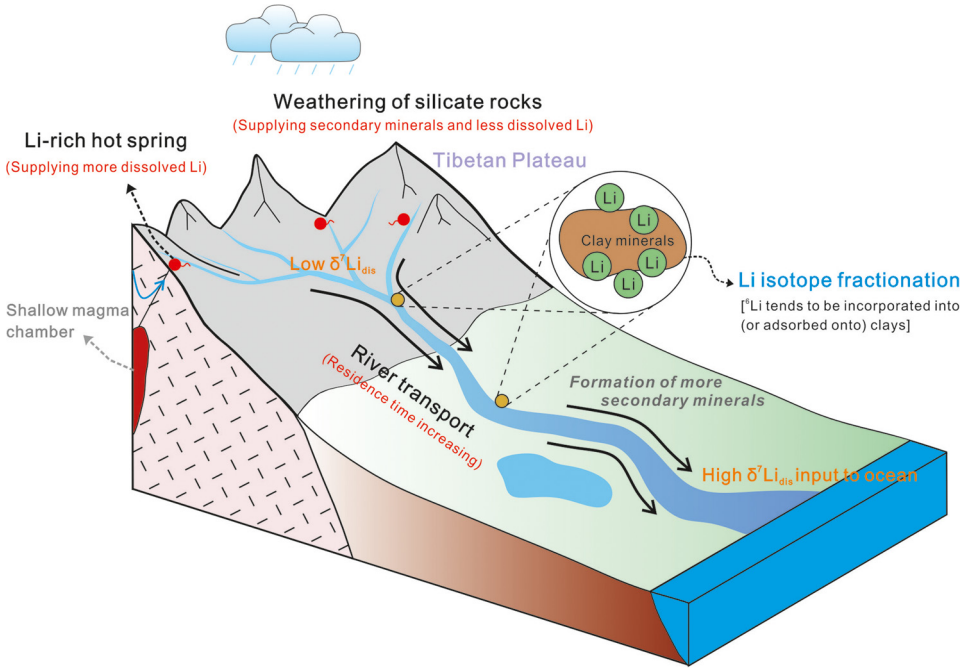

Fig. 9. A conceptual model for the source and fractionation of dissolved Li in rivers originated from the TP.

times. Consequently, the increase in dissolved Li flux and δ^7Li_{dis} in river water associated with continental geothermal water may have significantly contributed to the increased seawater δ^7Li in the Late Cenozoic.

CRediT authorship contribution statement

Jun-Wen Zhang: Data curation, Formal analysis, Investigation, Methodology, Resources, Writing – original draft, Writing – review & editing. **Ya-Ni Yan:** Formal analysis, Methodology, Resources, Writing – original draft, Writing – review & editing. **Zhi-Qi Zhao:** Conceptualization, Formal analysis, Funding acquisition, Investigation, Project administration, Resources, Supervision, Validation, Writing – original draft, Writing – review & editing. **Xiao-Ming Liu:** Conceptualization, Formal analysis, Validation, Writing – original draft, Writing – review & editing. **Xiao-Dong Li:** Formal analysis, Validation, Writing – original draft, Writing – review & editing. **Dong Zhang:** Formal analysis, Funding acquisition, Investigation, Writing – original draft, Writing – review & editing. **Hu Ding:** Investigation, Writing – original draft. **Jun-Lun Meng:** Investigation, Writing – original draft. **Cong-Qiang Liu:** Conceptualization, Formal analysis, Funding acquisition, Investigation, Project administration, Resources, Supervision, Validation, Writing – original draft, Writing – review & editing.

Declaration of competing interest

The authors declare that they have no known competing financial interests or personal relationships that could have appeared to influence the work reported in this paper.

Data availability

Data will be made available on request.

Acknowledgements

We thank Liu Taoze, Cui Lifeng, Gao Shuang, Jia Guodong, Zhang Xiaolong, Yang Ye, Liu Xu, and Ye Runcheng for helping with field work. We thank Shi Xiaonan for proving the monthly SPM data and Ye Zuxin for helping with the graphic works. We thank Dr. Philip A.E. Pogge von Strandmann and an anonymous reviewer for suggesting significant improvements to this manuscript. This work was supported by the National Natural Science Foundation of China (No. 41930863, 42003007, 42073009), Special Fund for Basic Scientific Research of Central Colleges, Chang'an University (No. 300102278302, 300102272102), and Opening Fund of the State Key Laboratory of Environmental Geochemistry (SKLEG2022205).

Appendix A. Supplementary material

Supplementary material related to this article can be found online at https://doi.org/10.1016/j.epsl.2022.117875.

References

Armijo, R., Tapponnier, P., Mercier, J.L., Han, T.L., 1986. Quaternary extension in southern Tibet: field observations and tectonic implications. J. Geophys. Res., Solid Earth 91 (B14), 13803–13872.

Bagard, M.L., West, A.J., Newman, K., Basu, A.R., 2015. Lithium isotope fractionation in the Ganges–Brahmaputra floodplain and implications for groundwater impact on seawater isotopic composition. Earth Planet. Sci. Lett. 432, 404–414.

Bernal, N.F., Gleeson, S.A., Dean, A.S., Liu, X.M., Hoskin, P., 2014. The source of halogens in geothermal fluids from the Taupo Volcanic Zone, North Island, New Zealand. Geochim. Cosmochim. Acta 126, 265–283.

Bohlin, M.S., Bickle, M.J., 2019. The reactive transport of Li as a monitor of weathering processes in kinetically limited weathering regimes. Earth Planet. Sci. Lett. 511, 233–243.

Caves Rugenstein, J.K., Ibarra, D.E., von Blanckenburg, F., 2019. Neogene cooling driven by land surface reactivity rather than increased weathering fluxes. Nature 571 (7763), 99–102.

Chan, L.H., Edmond, J.M., Thompson, G., 1993. A lithium isotope study of hot springs and metabasalts from mid-ocean ridge hydrothermal systems. J. Geophys. Res., Solid Earth 98 (B6), 9653–9659.

Choi, H.B., Ryu, J.S., Shin, W.J., Vigier, N., 2019. The impact of anthropogenic inputs on lithium content in river and tap water. Nat. Commun. 10 (1), 1–7.

Dellinger, M., Gaillardet, J., Bouchez, J., Calmels, D., Louvat, P., Dosseto, A., Gorge, C., Alanoca, L., Maurice, L., 2015. Riverine Li isotope fractionation in the Amazon River basin controlled by the weathering regimes. Geochim. Cosmochim. Acta 164, 71–93.

Foustoukos, D.I., James, R.H., Berndt, M.E., Seyfried Jr, W.E., 2004. Lithium isotopic systematics of hydrothermal vent fluids at the Main Endeavour Field, Northern Juan de Fuca Ridge. Chem. Geol. 212 (1–2), 17–26.

Galy, A., France-Lanord, C., Derry, L.A., 1999. The strontium isotopic budget of Himalayan rivers in Nepal and Bangladesh. Geochim. Cosmochim. Acta 63 (13–14), 1905–1925.
Godfrey, L.V., Chan, L.H., Alonso, R.N., Lowenstein, T.K., McDonough, W.F., Houston, J., Bobst, A., Jordan, T.E., 2013. The role of climate in the accumulation of lithium-rich brine in the Central Andes. Appl. Geochem. 38, 92–102.
Gou, L.F., Jin, Z., Pogge von Strandmann, P.A.E., Li, G., Qu, Y.X., Xiao, J., Deng, L., Galy, A., 2019. Li isotopes in the middle Yellow River: seasonal variability, sources and fractionation. Geochim. Cosmochim. Acta 248, 88–108.
He, M., Zheng, H., Huang, X., Jia, J., Li, L., 2013. Yangtze River sediments from source to sink traced with clay mineralogy. J. Asian Earth Sci. 69, 60–69.
Henchiri, S., Clergue, C., Dellinger, M., Gaillardet, J., Louvat, P., Bouchez, J., 2014. The influence of hydrothermal activity on the Li isotopic signature of rivers draining volcanic areas. Proc. Earth Planet. Sci. 10, 223–230.
Hindshaw, R.S., Teisserenc, R., Le Dantec, T., Tananaev, N., 2019a. Seasonal change of geochemical sources and processes in the Yenisei River: a Sr, Mg and Li isotope study. Geochim. Cosmochim. Acta 255, 222–236.
Hindshaw, R.S., Tosca, R., Goût, T.L., Farnan, I., Tosca, N.J., Tipper, E.T., 2019b. Experimental constraints on Li isotope fractionation during clay formation. Geochim. Cosmochim. Acta 250, 219–237.
Huh, Y., Chan, L.H., Zhang, L., Edmond, J.M., 1998. Lithium and its isotopes in major world rivers: implications for weathering and the oceanic budget. Geochim. Cosmochim. Acta 62 (12), 2039–2051.
Kısakürek, B., James, R.H., Harris, N.B.W., 2005. Li and δ^7Li in Himalayan rivers: proxies for silicate weathering?. Earth Planet. Sci. Lett. 237 (3–4), 387–401.
Li, G., West, A.J., 2014. Evolution of Cenozoic seawater lithium isotopes: coupling of global denudation regime and shifting seawater sinks. Earth Planet. Sci. Lett. 401, 284–293.
Li, J., Wang, X., Ruan, C., Sagoe, G., Li, J., 2022. Enrichment mechanisms of lithium for the geothermal springs in the southern Tibet, China. J. Hydrol. 128022.
Li, W., Liu, X.M., 2020. Experimental investigation of lithium isotope fractionation during kaolinite adsorption: implications for chemical weathering. Geochim. Cosmochim. Acta 284, 156–172.
Li, W., Liu, X.M., 2022. Mineralogy and fluid chemistry controls on lithium isotope fractionation during clay adsorption. Sci. Total Environ. 158138.
Liu, C.Q., Zhao, Z.Q., Wang, Q., Gao, B., 2011. Isotope compositions of dissolved lithium in the rivers Jinshajiang, Lancangjiang, and Nujiang: implications for weathering in Qinghai-Tibet Plateau. Appl. Geochem. 26, S357–S359.
Liu, X.M., Wanner, C., Rudnick, R.L., McDonough, W.F., 2015. Processes controlling δ^7Li in rivers illuminated by study of streams and groundwaters draining basalts. Earth Planet. Sci. Lett. 409, 212–224.
Ma, T., Weynell, M., Li, S.L., Liu, Y., Chetelat, B., Zhong, J., Xu, S., Liu, C.Q., 2020. Lithium isotope compositions of the Yangtze River headwaters: weathering in high-relief catchments. Geochim. Cosmochim. Acta 280, 46–65.
Maffre, P., Goddéris, Y., Vigier, N., Moquet, J.S., Carretier, S., 2020. Modelling the riverine δ^7Li variability throughout the Amazon Basin. Chem. Geol. 532, 119336.
Manaka, T., Araoka, D., Yoshimura, T., Hossain, H.Z., Nishio, Y., Suzuki, A., Kawahata, H., 2017. Downstream and seasonal changes of lithium isotope ratios in the Ganges-Brahmaputra river system. Geochem. Geophys. Geosyst. 18 (8), 3003–3015.
Millot, R., Négrel, P., 2007. Multi-isotopic tracing (δ^7Li, δ^{11}B, ^{87}Sr/^{86}Sr) and chemical geothermometry: evidence from hydro-geothermal systems in France. Chem. Geol. 244 (3–4), 664–678.
Millot, R., Scaillet, B., Sanjuan, B., 2010. Lithium isotopes in island arc geothermal systems: Guadeloupe, Martinique (French West Indies) and experimental approach. Geochim. Cosmochim. Acta 74 (6), 1852–1871.
Millot, R., Hegan, A., Négrel, P., 2012. Geothermal waters from the Taupo volcanic zone, New Zealand: Li, B and Sr isotopes characterization. Appl. Geochem. 27 (3), 677–688.
Misra, S., Froelich, P.N., 2012. Lithium isotope history of Cenozoic seawater: changes in silicate weathering and reverse weathering. Science 335 (6070), 818–823.
Murphy, M.J., Porcelli, D., Pogge von Strandmann, P.A.E., Hirst, C.A., Kutscher, L., Katchinoff, J.A., Mörth, C.-M., Maximov, T., Andersson, P.S., 2019. Tracing silicate weathering processes in the permafrost-dominated Lena River watershed using lithium isotopes. Geochim. Cosmochim. Acta 245, 154–171.
Penniston-Dorland, S., Liu, X.M., Rudnick, R.L., 2017. Lithium isotope geochemistry. Rev. Mineral. Geochem. 82 (1), 165–217.
Pogge von Strandmann, P.A.E., Henderson, G.M., 2015. The Li isotope response to mountain uplift. Geology 43 (1), 67–70.
Pogge von Strandmann, P.A.E., Burton, K.W., James, R.H., van Calsteren, P., Gíslason, S.R., Mokadem, F., 2006. Riverine behaviour of uranium and lithium isotopes in an actively glaciated basaltic terrain. Earth Planet. Sci. Lett. 251 (1–2), 134–147.
Pogge von Strandmann, P.A.E., Frings, P.J., Murphy, M.J., 2017. Lithium isotope behaviour during weathering in the Ganges Alluvial Plain. Geochim. Cosmochim. Acta 198, 17–31.
Pogge von Strandmann, P.A.E., Kasemann, S.A., Wimpenny, J.B., 2020. Lithium and lithium isotopes in Earth's surface cycles. Elem., Int. Mag. Miner. Geochem. Petrol. 16 (4), 253–258.
Pogge von Strandmann, P.A.E., Burton, K.W., Opfergelt, S., Genson, B., Guicharnaud, R.A., Gislason, S.R., 2021. The lithium isotope response to the variable weathering of soils in Iceland. Geochim. Cosmochim. Acta 313, 55–73.
Pogge von Strandmann, P.A.E., Liu, X., Liu, C.Y., Wilson, D.J., Hammond, S.J., Tarbuck, G., Aristilde, L., Krause, A.J., Fraser, W.T., 2022. Lithium isotope behaviour during basalt weathering experiments amended with organic acids. Geochim. Cosmochim. Acta 328, 37–57.
Raymo, M.E., Ruddiman, W.F., 1992. Tectonic forcing of late Cenozoic climate. Nature 359, 117.
Rudnick, R.L., Gao, S., 2003. Composition of the continental crust. In: Rudnick, R.L. (Ed.), Treatise in Geochemistry: The Crust. Elsevier, Oxford, pp. 1–64.
Sauzéat, L., Rudnick, R.L., Chauvel, C., Garçon, M., Tang, M., 2015. New perspectives on the Li isotopic composition of the upper continental crust and its weathering signature. Earth Planet. Sci. Lett. 428, 181–192.
Shi, X., Zhang, F., Lu, X., Wang, Z., Gong, T., Wang, G., Zhang, H., 2018. Spatiotemporal variations of suspended sediment transport in the upstream and midstream of the Yarlung Tsangpo River (the upper Brahmaputra), China. Earth Surf. Process. Landf. 43 (2), 432–443.
Steinhoefel, G., Brantley, S.L., Fantle, M.S., 2021. Lithium isotopic fractionation during weathering and erosion of shale. Geochim. Cosmochim. Acta 295, 155–177.
Teng, F.Z., McDonough, W.F., Rudnick, R.L., Dalpé, C., Tomascak, P.B., Chappell, B.W., Gao, S., 2004. Lithium isotopic composition and concentration of the upper continental crust. Geochim. Cosmochim. Acta 68 (20), 4167–4178.
Teng, F.Z., Rudnick, R.L., McDonough, W.F., Wu, F.Y., 2009. Lithium isotopic systematics of A-type granites and their mafic enclaves: further constraints on the Li isotopic composition of the continental crust. Chem. Geol. 262, 370–379.
Tomascak, P.B., Hemming, N.G., Hemming, S.R., 2003. The lithium isotopic composition of waters of the Mono Basin, California. Geochim. Cosmochim. Acta 67 (4), 601–611.
Vigier, N., Goddéris, Y., 2015. A new approach for modeling Cenozoic oceanic lithium isotope paleo-variations: the key role of climate. Clim. Past 11 (4), 635–645.
Vigier, N., Decarreau, A., Millot, R., Carignan, J., Petit, S., France-Lanord, C., 2008. Quantifying Li isotope fractionation during smectite formation and implications for the Li cycle. Geochim. Cosmochim. Acta 72 (3), 780–792.
Wang, Q.L., Chetelat, B., Zhao, Z.Q., Ding, H., Li, S.L., Wang, B.L., Li, J., Liu, X.L., 2015. Behavior of lithium isotopes in the Changjiang River system: sources effects and response to weathering and erosion. Geochim. Cosmochim. Acta 151, 117–132.
Wanner, C., Sonnenthal, E.L., Liu, X.M., 2014. Seawater δ^7Li: a direct proxy for global CO_2 consumption by continental silicate weathering? Chem. Geol. 381, 154–167.
Weynell, M., Wiechert, U., Schuessler, J.A., 2017. Lithium isotopes and implications on chemical weathering in the catchment of Lake Donggi Cona, northeastern Tibetan Plateau. Geochim. Cosmochim. Acta 213, 155–177.
Weynell, M., Wiechert, U., Schuessler, J.A., 2021. Lithium isotope signatures of weathering in the hyper-arid climate of the western Tibetan Plateau. Geochim. Cosmochim. Acta 293, 205–223.
Winnick, M.J., Druhan, J.L., Maher, K., 2022. Weathering intensity and lithium isotopes: a reactive transport perspective. Am. J. Sci. 322 (5), 647–682.
Xu, Z., Li, T., Li, G., Hedding, D.W., Wang, Y., Gou, L.F., Zhao, L., Chen, J., 2021. Lithium isotopic composition of soil pore water: responses to evapotranspiration. Geology 50 (2), 194–198.
Yoshimura, T., Araoka, D., Kawahata, H., Hossain, H.M., Ohkouchi, N., 2021. The influence of weathering, water sources, and hydrological cycles on lithium isotopic compositions in river water and groundwater of the Ganges–Brahmaputra–Meghna River system in Bangladesh. Front. Earth Sci. 9, 535.
Zhang, F., Dellinger, M., Hilton, R.G., Yu, J., Allen, M.B., Densmore, A.L., Sun, H., Jin, Z., 2022. Hydrological control of river and seawater lithium isotopes. Nat. Commun. 13 (1), 1–10.
Zhang, J.W., Yan, Y.N., Zhao, Z.Q., Li, X.D., Guo, J.Y., Ding, H., Cui, L.F., Meng, J.L., Liu, C.Q., 2021a. Spatial and seasonal variations of dissolved arsenic in the Yarlung Tsangpo River, southern Tibetan Plateau. Sci. Total Environ. 760, 143416.
Zhang, J.W., Zhao, Z.Q., Yan, Y.N., Cui, L.F., Wang, Q.L., Meng, J.L., Li, X.D., Liu, C.Q., 2021b. Lithium and its isotopes behavior during incipient weathering of granite in the eastern Tibetan Plateau, China. Chem. Geol. 559, 119969.
Zhang, L., Chan, L.H., Gieskes, J.M., 1998. Lithium isotope geochemistry of pore waters from Ocean Drilling Program Sites 918 and 919, Irminger Basin. Geochim. Cosmochim. Acta 62 (14), 2437–2450.